Fundamentals of Radiometry and Photometry

Prof. Elias N. Glytsis

March 23, 2021

School of Electrical & Computer Engineering
National Technical Univerity of Athens

This page was intentionally left blank.....

Contents

This page was intentionally left blank.....

1. Radiometry and Photometry

1.1. Introduction

Radiometry is the process of measuring electromagnetic radiation. Radiometry deals with the measurement of the energy transferred by a source through a medium (or media) to a receiver. In radiometry, radiation of all wavelengths in the electromagnetic spectrum (see Fig. 1) is treated equally. Traditionally, radiometry uses the laws of geometrical optics in order to treat the propagation of energy from a source to the surrounding space [1]. This treatment is equivalent to assuming that the energy flow is achieved via incoherent electromagnetic fields. The complexity that is added due to the degree of coherence as well as due to the interference and diffraction effects, is not necessary in most of radiometry problems [1].

Radiometry is divided according to various regions of the electromagnetic spectrum for which similar measurement techniques can be applied. Therefore, ultraviolet radiometry, intermediate-infrared radiometry, far-infrared radiometry and microwave radiometry are considered separate fields. However, all radiometries are distinguished from the radiometry in the visible and near-visible region of the electromagnetic spectrum. This subdivision of radiometry that deals with the measurement of the electromagnetic radiation in the visible range and near-visible part of the electromagnetic spectrum, is called *Photometry* and is based on the human perception of light.

1.2. Basic Radiometric and Photometric Quantities

An important part of the design of an optical system is its efficiency in transferring light. One must be able to specify the amount of energy emitted or received. Many similar quantities are used to specify the amount of light (electromagnetic radiation in general) leaving a source or arriving at a receiver, and many different systems of units are used. In this section, all quantities related to radiometry have the adjective *radiant* and carry the subscript "e" (for electromagnetic). On the other hand all quantities related to photometry have the adjective *luminous* and carry the subscript "v" (for visible). The basic radiometric and photometric quantities are the radiant/luminous energy (Q_e and Q_v respectively), the radiant/luminous power (Φ_e and Φ_v respectively), the radiant/luminous intensity (I_e and I_v respectively), the radiance/luminance (L_e and L_v respectively), the irradiance/illuminance (E_e and E_v respectively), and the radiant/luminous emittance (M_e and M_v respectively). The radiant/luminous intensity, the radiance/luminance, and the radiant/luminous emittance are usually associated with sources. On the other hand the irradiance/illuminance are usually associated with receivers of radiation.

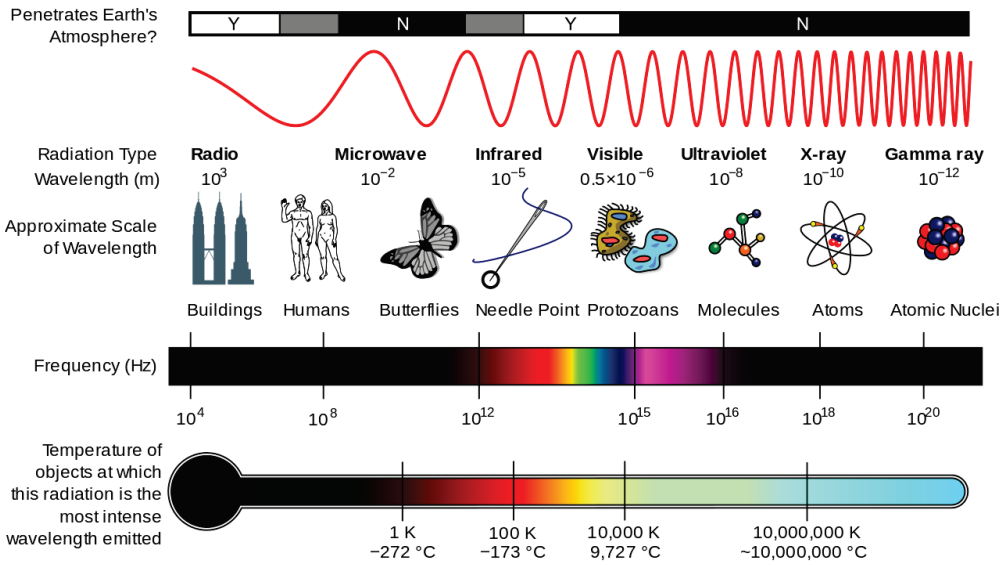

Figure 1: The electromagnetic spectrum from the radio-wave regime up to the gamma-ray regime. (from url-link: https://en.wikipedia.org/wiki/Electromagnetic_spectrum).

All these quantities definitions and their corresponding SI (System International) units are summarized in Table 1. In the definitions of Table 1, $d\Omega$ is the differential solid angle, dA_s is the differential area of an extended sourse, $dA_{s\perp}$ is the projected sourse area in a direction of observation ($dA_{s\perp} = dA_s \cos\theta$ where θ is the observation angle from the normal of the source surface). More details on this area and corresponding angle will be presented later. For the photometric quantities and especially for illuminance and luminance there are many other non-SI units. The most important of those other units are summarized in Table 2 for information purposes.

1.3. Point Source

A point light source (inside an isotropic homogeneous medium) usually radiates energy isotropically in the surrounding space. Therefore its intensity $I = d\Phi/d\Omega$ can be considered constant. A simple representation of a point light source is shown in Fig. 2, and its intensity is given by

$$I = \frac{d\Phi}{d\Omega} = \frac{\Phi}{\Omega}, \tag{1}$$

where I is the constant intensity (could be either radiant or luminous).

Now consider a planar surface at distance R from an isotropic point source of intensity I as shown in Fig. 3. The irradiance (or illuminance) at various points of the planar surface

Table 1: Radiometric and Photometric Quantities

Radiometric				**Photometric**		
Quantity	**Symbol**	**Unit**	**Definition**	**Quantity**	**Symbol**	**Unit**
Radiant Energy	Q_e	Joule		Luminous Energy	Q_v	Talbot
Radiant Power	Φ_e	Watt	$\Phi = \frac{dQ}{dt}$	Luminous Power	Φ_v	Lumen (lm)
Radiant Intensity	I_e	$\frac{\text{Watt}}{\text{sr}}$	$I = \frac{d\Phi}{d\Omega}$	Luminous Intensity	I_v	candela cd $= \frac{\text{lm}}{\text{sr}}$
Radiance	L_e	$\frac{\text{Watt}}{\text{m}^2\text{sr}}$	$L = \frac{d^2\Phi}{d\Omega dA_{s\perp}}$	Luminance	L_v	$\frac{\text{lm}}{\text{m}^2\text{sr}}$
Irradiance	E_e	$\frac{\text{Watt}}{\text{m}^2}$	$E = \frac{d\Phi}{dA}$	Illuminance	E_v	Lux $= \frac{\text{lm}}{\text{m}^2}$
Radiant Exitance	M_e	$\frac{\text{Watt}}{\text{m}^2}$	$M = \frac{d\Phi}{dA_s}$	Luminous Exitance	M_v	$\frac{\text{lm}}{\text{m}^2}$

Table 2: Common Non-SI units of Illuminance and Luminance

Quantity	**SI unit**	**Non-SI Unit**	**Conversion to SI (K)** (non-SI unit) = K (SI unit)
Illuminance, E_v	Lux	Phot	10000
		Footcandle	10.764
Luminance, L_v	cd/m^2	Stilb	10000
		Apostilb	$1/\pi = 0.3183$
		Lambert	$10^4/\pi = 3183$
		MilliLambert	$10/\pi = 3.183$
		FootLambert	3.426
		Nit	1
		Skot	$10^{-3}/\pi$
		cd/ft^2	10.764
		cd/in^2	1550

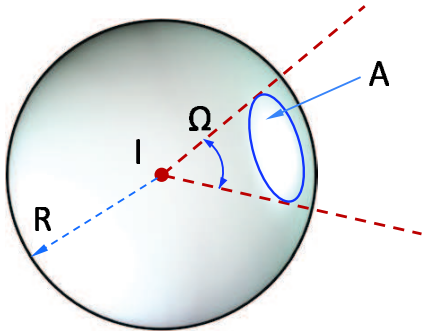

Figure 2: A point light source emitting radiation isotropically into surrounding space. The intensity of the point source is I.

is sought. Consider a differential area dA which is at the angle $\theta = 0$ (just against the point source). The irradiance received by this area is given by

$$E(\theta = 0) = \frac{d\Phi}{dA} = \frac{d\Phi}{R^2 d\Omega} = \frac{d\Phi}{d\Omega}\frac{1}{R^2} = \frac{I}{R^2} = E_0. \tag{2}$$

Now the irradiance at a differential area that is located at a direction specified by the angle θ is sought. Assume that the differential area on the planar surface is dA' (see Fig. 3). Then the irradiace due to the point source at this position can be determined as follows

$$E(\theta, \phi) = \frac{d\Phi'}{dA'} = \frac{d\Phi'}{dA/\cos\theta} = \frac{d\Phi'}{d\Omega' R'^2}\cos\theta = \frac{I}{R^2/\cos^2\theta}\cos\theta = \frac{I}{R^2}\cos^3\theta = E_0\cos^3\theta. \tag{3}$$

The last equation reveals a fall-off of the received irradiance on the plane that is governed by the $cos^3\theta$ term. The fall-off is shown in Fig. 4 where the simple cosine fall-off is also shown as a reference. Due to the isotropic behavior of the point source the irradiance is independent of the azimuthal angle ϕ.

1.4. Extended Source

For an extended source the significant quantity is the radiance/luminance. The radiance (or luminance), L, can be defined based on the geometric configuration of Fig. 5 as

$$L = \frac{d^2\Phi}{d\Omega dA_{s\perp}} = \frac{d^2\Phi}{d\Omega dA_s\cos\theta} = \frac{dI}{dA_s\cos\theta}. \tag{4}$$

From the previous definition it is evident that when an extended source is observed at a grazing angle (i.e., when $\theta \to \pi/2$) the radiance/luminance tends to infinity which means that the source will look brighter and brighter as it is observed at larger angles θ. However, this is

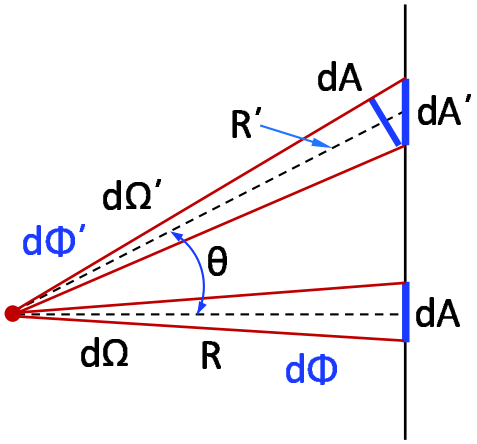

Figure 3: A point light source emitting radiation in front of a planar surface.

contradictory to everyday practice where extended sources usually look dimmer when they are observed at angles close to grazing angle. A special case is when the radiance/luminance is independent of the angle θ. An extended source that has a constant radiance/luminance is defined as a *Lambertian source*. In order for this to occur a Lambertian source's intensity should be given by $I(\theta) = I_0 \cos\theta$. Therefore, for a Lambertian source, the intensity and radiance are given by

$$I(\theta) = I_0 \cos\theta, \tag{5}$$

$$L(\theta) = L_0, \tag{6}$$

where I_0 and L_0 are constants. A polar plot of the intensity and radiance of a Lambertian source is shown in Fig. 6.

Now consider a planar surface at distance R from an extended source of radiance L as shown in Fig. 7. The irradiance/illuminance at various points of the planar surface is sought. Consider a differential area dA which is at the angle $\theta = 0$ (just against the extended source). Also consider an elementary area dA_s of the extended source.

The irradiance dE received at the plane on the area dA is given by

$$dE(\theta = 0) = \frac{d^2\Phi}{dA} = \frac{L d\Omega dA_s}{dA} = L \frac{dA}{R^2} \frac{dA_s}{dA} = L \frac{dA_s}{R^2}. \tag{7}$$

If the extended source is Lambertian and has a size with dimensions much smaller than the distance from the planar surface R, then the last equation can be integrated as follows

$$E(\theta = 0) = E_0 = \int_{A_s} L \frac{dA_s}{R^2} = L \int_{A_s} \frac{dA_s}{R^2} \simeq L\Omega, \tag{8}$$

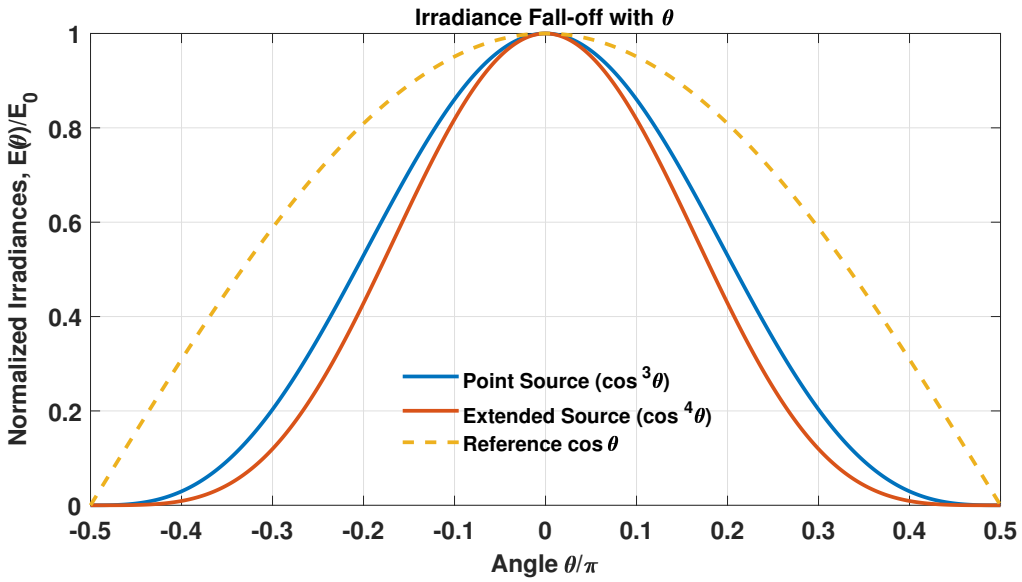

Figure 4: The fall-off of irradiance as a function of the angle θ for a point source and an extended source. The cosine curve is shown for reference purposes.

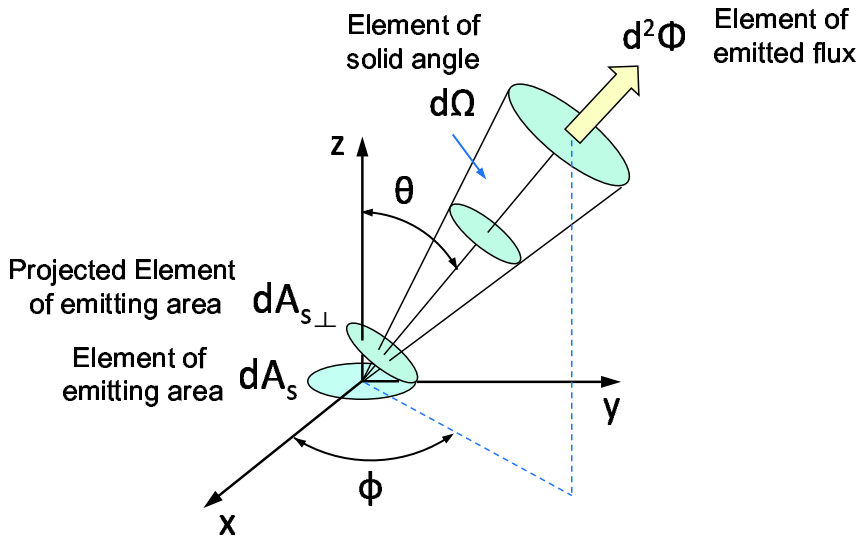

Figure 5: An extended source of differential element dA_s, emitting radiation flux of $d^2\Phi$ inside a solid angle $d\Omega$. The differential element $dA_{s\perp}$ corresponds to the projected emitting area in the direction specified by the azimuthal angle ϕ and the polar angle θ.

where Ω is the solid angle by which the extended source area is subtended from the center of dA. The irradiance at the infinitesimal area dA' can be determined as follows

$$dE(\theta) = \frac{d^2\Phi'}{dA'} = \frac{Ld\Omega' dA_s \cos\theta}{dA'} = L\,\frac{dA'\cos\theta}{R'^2}\frac{dA_s\cos\theta}{dA'} = L\,\frac{dA_s}{R^2}\cos^4\theta, \tag{9}$$

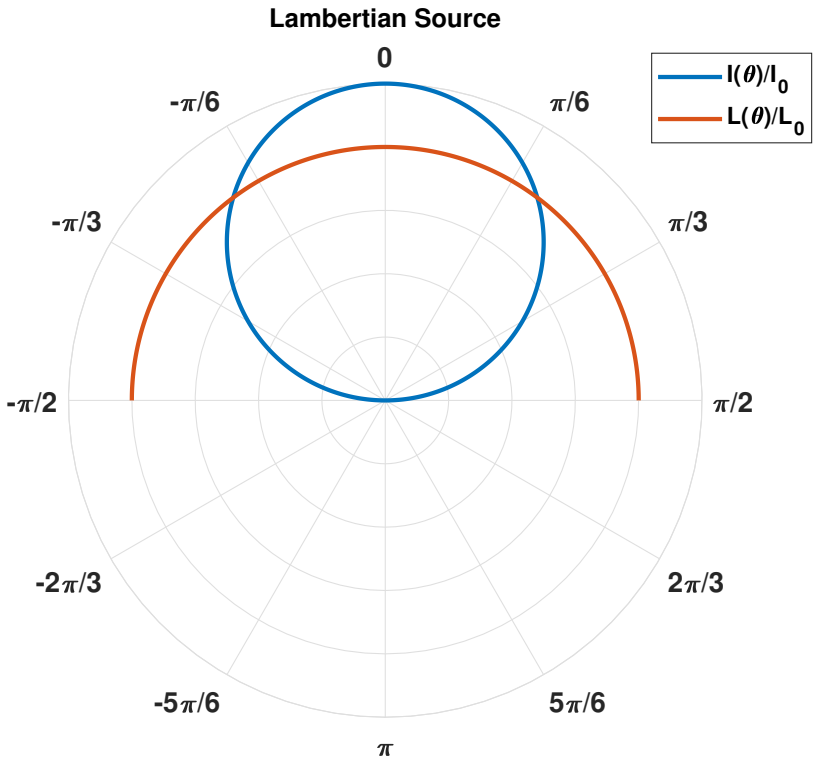

Figure 6: The normalized intensity $I(\theta)/I_0$ and the normalized radiance $L(\theta)/L_0$ of a Lambertian source in a polar diagram.

where in the last equation the relation $R' = R/\cos\theta$ was utilized. Assuming again that the extended source is Lambertian and of dimensions much smaller than the distance R the irradiance at the plane in the direction of θ is given by

$$E(\theta) = \int_{A_s} L \, \frac{dA_s}{R^2} \cos^4\theta = L \int_{A_s} \frac{dA_s}{R^2} \cos^4\theta \simeq L\Omega \cos^4\theta = E_0 \cos^4\theta. \tag{10}$$

The last equation is known as the irradiance cosine-fourth-power fall-off. Therefore, the irradiance of an extended Lambertian source falls more abruptly than the irradiance of a point source [that is falling with cosine-third-power as it is shown in Eq. (3)]. The fall-off is shown in Fig. 4 where the simple cosine fall-off is also shown as a reference along with the fall-off of a point source. Due to the Lambertian properties of the extended source and its small dimensions (compared to R) the irradiance is independent of the azimuthal angle ϕ.

1.5. Conservation Laws for Radiance/Luminance

Now let's consider an infinitesimal beam propagating inside a lossless isotropic and homogeneous medium as shown in Fig. 8. The beam is intersecting two fictitious infinitesimal

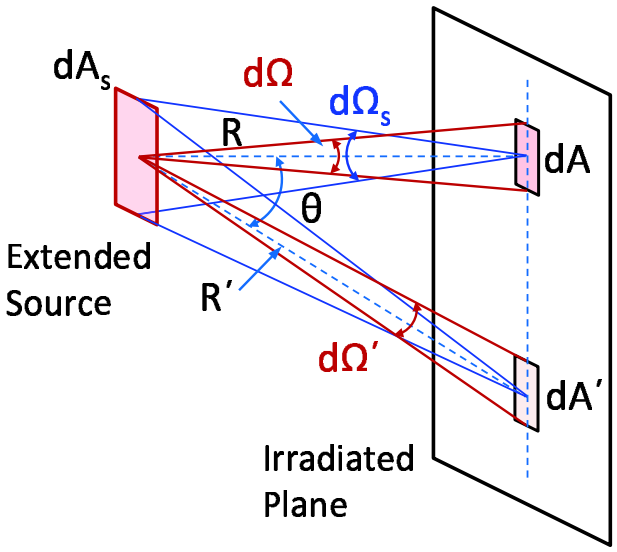

Figure 7: An extended light source emitting radiation in front of a planar surface.

surfaces dA_1 and dA_2 as shown. The areas are tilted with their normals forming angles of θ_1 and θ_2 with respect to the ray direction, respectively. Since the areas are infinitesimal there is no significant difference in radiance L_1 among rays diverging from any point of dA_1 and the radiance L_2 among rays converging to any point of dA_2 [2,3]. The radiant/luminous infinitesimal power (flux) $d^2\Phi_1$ of the beam leaving from surface dA_1 is given by

$$d^2\Phi_1 = L_1 dA_1 \cos\theta_1 d\Omega_1 = L_1 dA_1 \cos\theta_1 \left(\frac{dA_2 \cos\theta_2}{R^2}\right) = L_1 \frac{dA_1 dA_2 \cos\theta_1 \cos\theta_2}{R^2}. \tag{11}$$

Similarly, the radiant/luminous infinitesimal power $d^2\Phi_2$ of the beam leaving from surface dA_2 is given by

$$d^2\Phi_2 = L_2 dA_2 \cos\theta_2 d\Omega_2 = L_2 dA_2 \cos\theta_2 \left(\frac{dA_1 \cos\theta_1}{R^2}\right) = L_2 \frac{dA_2 dA_1 \cos\theta_2 \cos\theta_1}{R^2}. \tag{12}$$

However, due to the lossless medium the power should be conserved. Therefore, $d^2\Phi_1 = d^2\Phi_2$ and from the last two equations it is implied that

$$L_1 = L_2. \tag{13}$$

Because there was not any restriction imposed on the areas dA_1 and dA_2 of the beam and their centers C_1 and C_2 Eq. (13) must apply to any pair of points along the beam assuming a lossless, isotropic and homogeneous medium. This property is called *radiance/luminance invariance* or *radiance/luminance conservation* [2,3].

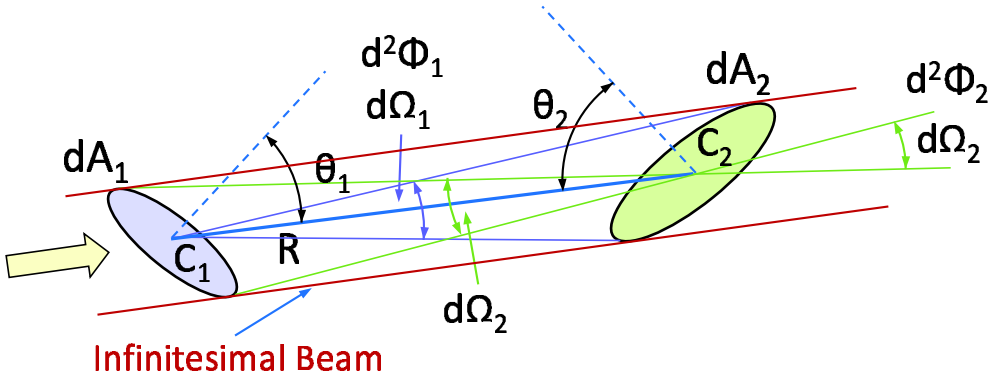

Figure 8: An infinitesimal beam carrying radiant/luminous flux inside a lossless isotropic and homogeneous medium. The beam is crossing two infinitesimal surfaces dA_1 and dA_2 separated by a distance R. The planes of the infinitesimal surfaces are at angles θ_1 and θ_2 with respect to their normals. The points C_1 and C_2 are the centers of the infinitesimal areas.

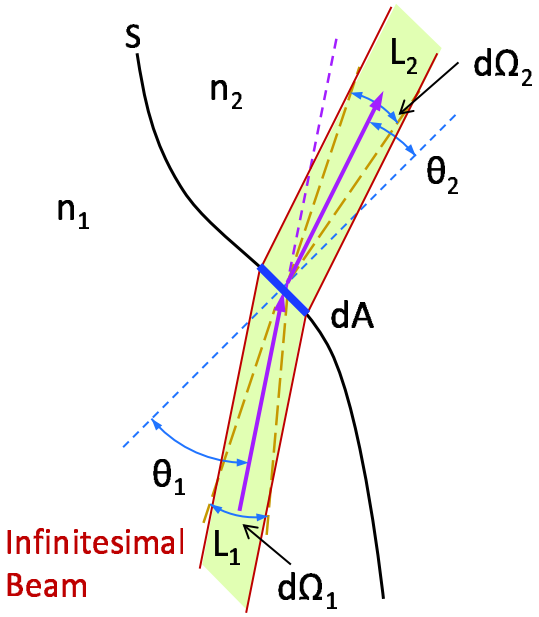

Figure 9: An infinitesimal beam carrying radiant/luminous flux refracting at the interface between two lossless isotropic and homogeneous media of refractive indices n_1 and n_2 respectively. The beam is crossing an infinitesimal surface dA at the boundary between the two media.

Next, the radiance conservation should be considered in the case that the beam is refracting at an interface between two different lossless isotropic and homogeneous media. The situation is depicted in Fig. 9. An infinitesimal area dA of the beam is shown on the smooth

boundary surface S between the two media [2]. Using the same arguments as previously the infinitesimal power incident on the area dA of the boundary is given by

$$d^2\Phi_1 = L_1 dA \cos\theta_1 d\Omega_1 = L_1 dA \cos\theta_1 \sin\theta_1 d\theta_1 d\phi, \tag{14}$$

where L_1 is the radiance/luminance from the side of dA facing medium of refractive index n_1 and ϕ is the azimuthal angle on the tangential plane to the boundary at the position of dA. Similarly, the power that is refracting into the medium of refractive index n_2 is given by

$$d^2\Phi_2 = L_2 dA \cos\theta_2 d\Omega_2 = L_2 dA \cos\theta_2 \sin\theta_2 d\theta_2 d\phi, \tag{15}$$

where L_2 is the radiance/luminance from the side of dA facing medium of refractive index n_2. If it is assumed that the power reflection coefficient at the boundary is ρ (for the angle of incidence θ_1) then the relation between $d^2\Phi_1$ and $d^2\Phi_2$ should be

$$\begin{aligned} d^2\Phi_2 &= (1-\rho) d^2\Phi_1 \Longrightarrow \\ L_2 dA \cos\theta_2 \sin\theta_2 d\theta_2 d\phi &= (1-\rho) L_1 dA \cos\theta_1 \sin\theta_1 d\theta_1 d\phi \Longrightarrow \\ L_2 \cos\theta_2 \sin\theta_2 d\theta_2 &= (1-\rho) L_1 \cos\theta_1 \sin\theta_1 d\theta_1. \end{aligned} \tag{16}$$

From Snell's law it is straightforward to show that $n_1 \cos\theta_1 d\theta_1 = n_2 \cos\theta_2 d\theta_2$. Using the Snell's law the last equation results in

$$\frac{L_2}{n_2^2} = (1-\rho)\frac{L_1}{n_1^2}, \tag{17}$$

where Eq. (17) represents the *radiance/luminance conservation via an interface*. In case that the reflections can be neglected (as it was done in the section of blackbody radiation) then $L_1/n_1^2 = L_2/n_2^2$. Of course if $n_1 = n_2$ Eq. (17) coincides to Eq. (13) ($\rho = 0$, since there is no refractive index change).

2. Basics of Photometry

Photometry is the radiometry that is associated with the visible and near visible part of the electromagnetic spectrum. Therefore, photometry is associated with the response of the human eye to light. In order to set the ground for photometry it is necessary to examine the response of the human eye to visible light. A simple diagram of the human eye is shown in Fig. 10. Light passes through the cornea, the iris, the eye lens, the aqueous humour, the vitrous humour and falls on the light sensitive retina (which constitutes the human photodetector). The retina contains two types of photoreceptors the *cone* cells and the *rod* cells. These photoreceptors convert the absorbed photon energy into electrochemical signals that through the optic nerve are transferred to the back of the human brain which performs the necessary processing to implement the sense of vision. The cone cells are primarily responsible for the day vision (which means good illumination conditions) while the rod cells are mainly responsible for the night vision (which means poor illumination conditions). The cone-based vision is called *photopic vision* while the rod-based vision is called *scotopic vision*. There is also an intermediate regime referred as *mesopic vision* in which both rod and cone cells operate and there is not a clear distinction between the role of cone and rod cells. A simple diagram of these vision regimes is shown in Fig. 11 (from Ref. [4]). In practice photopic vision is distinguished from scotopic vision by the luminance range in which it functions. Photopic vision usually prevails for luminances of about $3\,cd/m^2$ or higher and scotopic vision prevails for luminances of about $0.003\,cd/m^2$ or lower [5]. The mesopic vision regime is in between, i.e. for luminances between $0.003\,cd/m^2$ to $3\,cd/m^2$. However, as it implied from Fig. 11 these boundaries are fuzzy and depend on the individual. The more sensitive rod cells require at least 5-14 photons to respond at very low luminance values (they become insensitive when the luminance drops to about $10^{-6}\,cd/m^2$). Cones on the other hand require about 100-1000 photons before they respond [5]. By comparison, four or more photons are necessary to induce a reaction in the fine silver halide grains of high-speed photographic film. Therefore, human eye rod cells have a detectivity that compares well to that of photographic film. On the other hand, CCD arrays can have a sensitivity to about 1 photon/pixel/second distributed over the surface of a sensor having 1 million active pixels [6].

The rod cells are sensitive to a wider section of the visible spectrum. The cone cells are divided into three main types: (a) The red-type (R-type) cone cells (or equivalently long wavelength L-cone cells) which are more sensitive in the red-green part of the visible spectrum; (b) the green-type (G-type) cone cells (or equivalently medium wavelength M-cone cells) which are more sensitive in the green-blue part of the visible spectrum; and finally

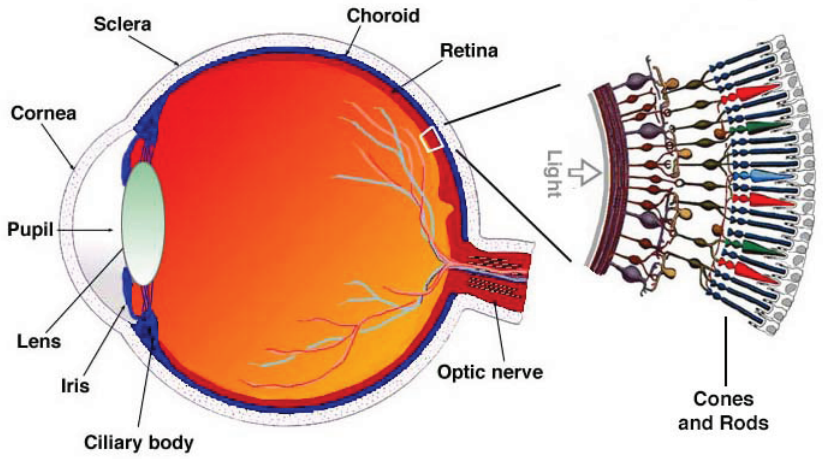

Figure 10: A diagram of the human eye with its photoreceptors (three types of cones and rods). (from url-link: http://www.blueconemonochromacy.org/how-the-eye-functions/).

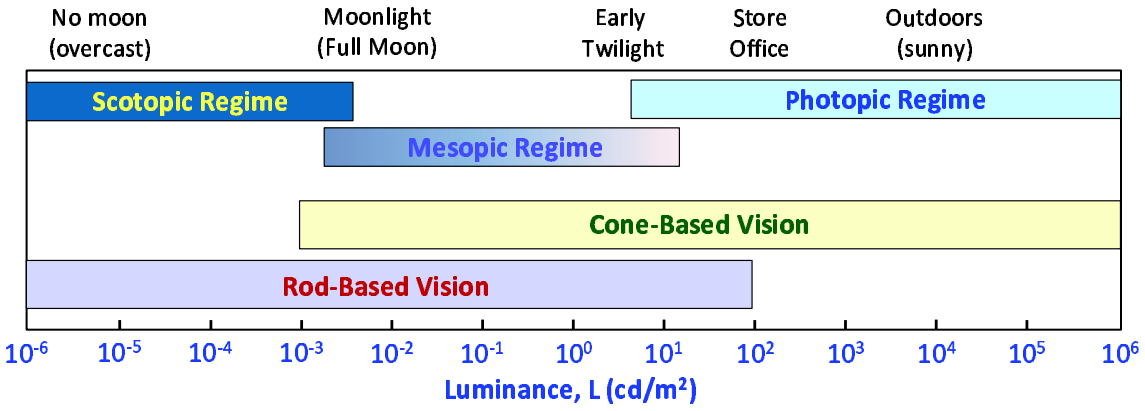

Figure 11: Approximate ranges of vision regimes (slightly modified from Ref. [4]).

(c) the blue-type (B-type) cone cells (or equivalently short wavelength S-cone cells) which are more sensitive in the blue-violet part of the visible spectrum. The rod and cone cells spectral sensitivity is revealed in their absorption characteristics in the visible spectrum and is shown in Fig. 12. The rod cells are more abundant in the retina and their peak density is at an angle from the central vision region (fovea centralis) while the cone cells are fewer and they are mostly concentrated in the central region of the retina. The fovea centralis is a narrow portion of the retina, about 1.5mm in diameter, in which the cone cells cones density is the highest. The cone and rod cell densities are shown in Fig. 13. Observe the

region of the optic nerve where there are no cone or rod cells (which is referred as the blind spot). There are approximately 100 millions rod cells and 7 millions cone cells on the average human eye [5]. The relative densities of the cone cells varies also depending on the cone cell type. The relative ratio of red-type, green-type, and blue-type cone cells is approximately 32:16:1 for the average human eye [5]. This means that there are many more red-type and green-type cone cells than blue-type cone cells.

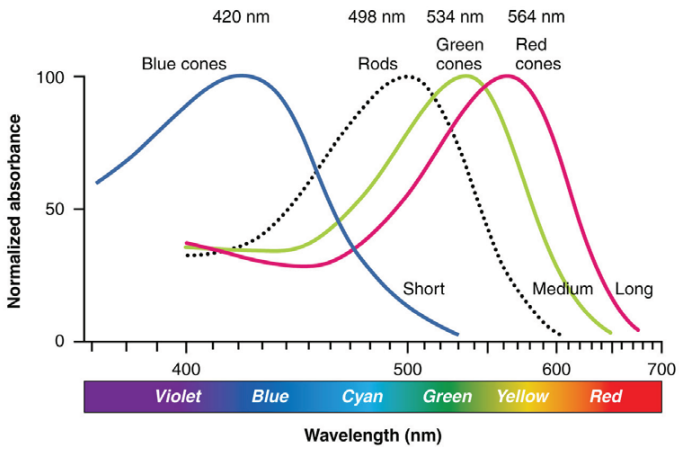

Figure 12: Normalized human photoreceptor absorbances for different wavelengths of light. (from url-link: https://en.wikipedia.org/wiki/Photoreceptor_cell).

2.1. Human Eye Response and Its Luminous Efficiency

The human eye is a photodetector that converts radiant energy (photons) into electrochemical signals that are processed by the human brain. As it was discussed previously, both cone cells and rod cells comprised the human photodetectors. The sensitivity of these cells was shown in Fig. 12. All these cells produce as an output a brightness and a color response. However, the response of the human eye is not determined by a physical measurement but by the sensation of brightness and colors that a human perceives to various light conditions. In order to measure the spectral sensation of the human eye a matching method was employed [5]. More specifically, a predetermined reference light of a specific wavelength was utilized in order for the luminous power Φ_v of a test light of arbitrary wavelength to match the sensation of the reference light. By measuring the radiant power Φ_e of the test light in the match conditions the luminous and the radiant powers can be related via the equation

$$\Phi_v = K\Phi_e, \tag{18}$$

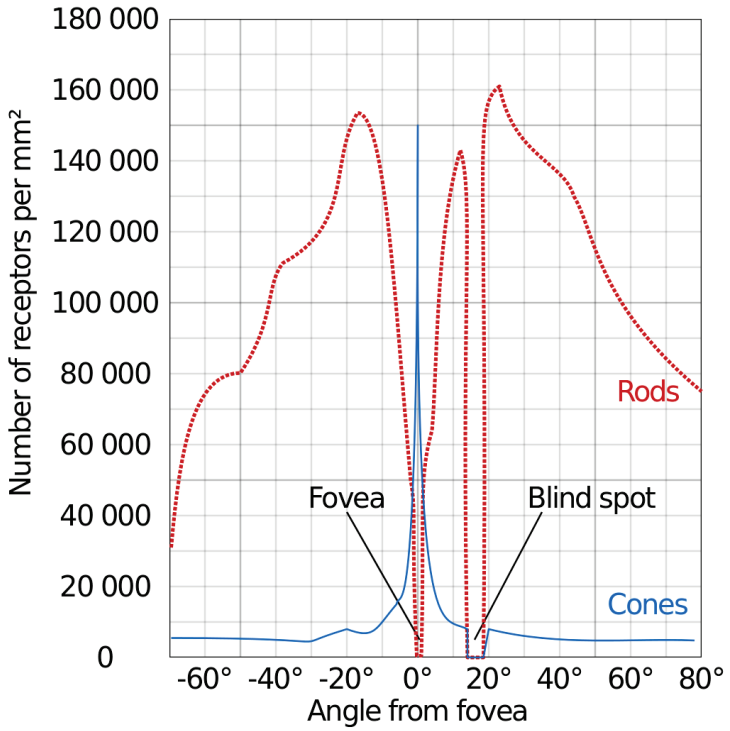

Figure 13: The density of photoreceptors (cones and rods) of the human eye. (from url-link: https://en.wikipedia.org/wiki/Photoreceptor_cell).

where K is a measure of the brightness sensation per unit radiant power and could be defined as the responsivity of the human eye. There are several methods to make the matching of the test light to the reference light [5]. However, the most common and practical is the flicker method. In this method a reference light of wavelength λ_{ref} and a test light of wavelength λ_{test} are alternating into the visual field of an individual and the perceived color could flicker. There is a frequency of alternating the two colors for which a flickering is observed in the perceived color when the brightness of the two lights differ. In this regime the brightness of the test light can be varied until there is no flickering in the perceived color by the alternation of the two colors in the visual field of the individual under test. For the setting where the flickering disappears the two lights are perceived to be matched. Based on this and similar techniques the value of K in Eq. (18) was determined. The K is called the luminous efficacy of radiation and is wavelength dependent $K(\lambda_0)$. If K_m is the maximum value of $K(\lambda_0)$ then $K(\lambda_0) = K_m V(\lambda_0)$ where $V(\lambda_0)$ is called *luminous efficiency*. Then the following equations

can be written

$$K(\lambda_0) = K_m V(\lambda_0), \tag{19}$$

$$K'(\lambda_0) = K'_m V'(\lambda_0), \tag{20}$$

where the non-primed variables correspond to photopic vision conditions and the primed variables to scotopic vision conditions respectively.

The standard photopic (or scotopic) luminous efficiency function $V(\lambda_0)$ [7, 8] (or $V'(\lambda_0)$ [9]) is based on a curious combination of measurement data from several sources and obtained by several methods. These luminous efficiencies are shown as functions of the freespace wavelength in Fig. 14. The uncertainty surrounding these functions (initially for $V(\lambda_0)$) is illustrated by the fact that the values from the different studies that were averaged to define it diverged by as much as a factor of ten in the violet [7, 10]. The standard luminous efficiency function $V(\lambda_0)$ seriously underestimates sensitivity at short wavelengths. The constants K_m and K'_m of Eqs. (19) and (20) have been set equal to $683\,lm/W$ and $1700\,lm/W$, respectively. The maximum of the $V(\lambda_0)$ luminous efficiency occurs at $\lambda_0 = 555\mu$m, while the maximum of $V'(\lambda_0)$ occurs at $\lambda_0 = 507\,\mu$m. Therefore, $683\,lm$ were set equal to one Watt of radiant power at the freespace wavelength of $\lambda_0 = 555\,\mu$m. Since, the initial data of luminous efficiency were published by CIE in 1924 there have been several improvements. However, for the purposes of this introductory material not any other curves will be described. The interest reader may refer to Refs. [5, 11] for additional information.

Equations (19) and (20) can be generalized for the conversion of the radiant power of a light source into luminous power. If $\Phi_e(\lambda_0)$ is the spectral radiant power of a light source then its luminous power is given by

$$\Phi_v = 683(lm/W)\int_{\lambda_0} \Phi_e(\lambda_0)V(\lambda_0)d\lambda_0, \qquad \text{Photopic Vision,} \tag{21}$$

$$\Phi_v = 1700(lm/W)\int_{\lambda_0} \Phi_e(\lambda_0)V'(\lambda_0)d\lambda_0, \qquad \text{Scotopic Vision,} \tag{22}$$

where the integral is over all the spectrum of the light source. For monochromatic sources (as they are nearly most of the lasers) $\Phi_e(\lambda_0) = P_0\delta(\lambda_0 - \lambda_{0L})$ and $\Phi_v = \kappa P_0 V(\lambda_{0L})$, where λ_{0L} is the wavelength of the monochromatic source and P_0 its corresponding power. The parameter $\kappa = 683\,lm/W$ or $1700\,lm/W$ for the photopic regime or the scotopic regime, respectively.

The situation for the mesopic vision regime is quite more complicated and there is not a standard luminous efficiency curve as the ones shown in Fig. 14 for photopic and scotopic regimes. However, some recent proposals [12, 13, 14] have been published in the literature

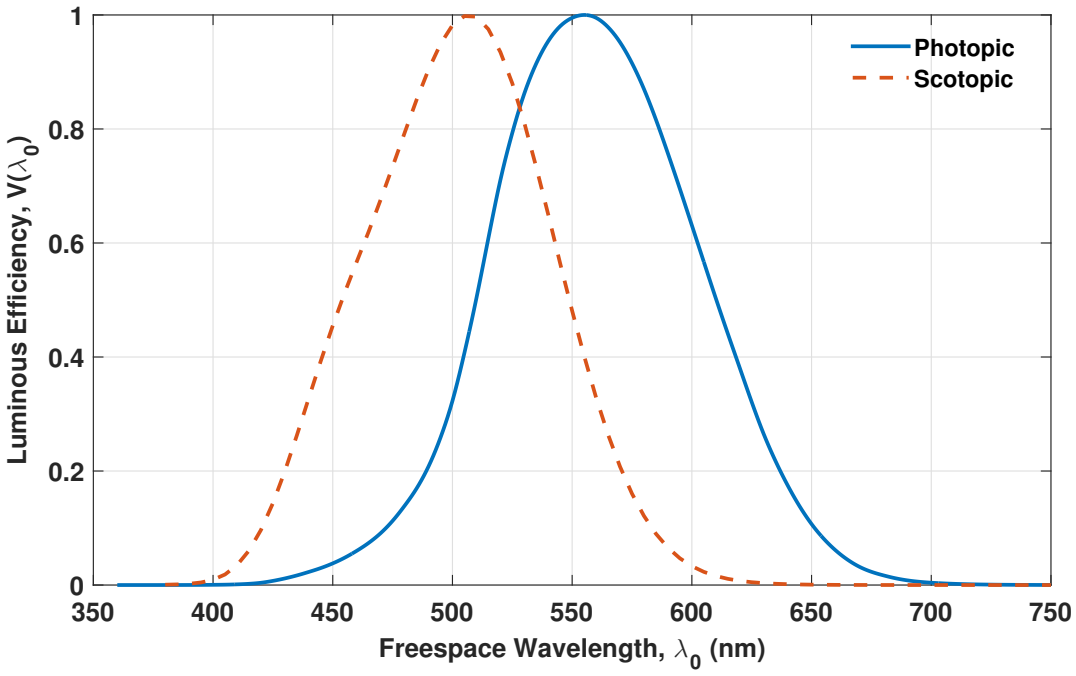

Figure 14: Luminous efficiency curve under good illumination conditions (photopic) and poor illumination conditions (scotopic).

regarding this issue. Based on Ref. [13] the mesopic luminous efficiency, $V_{mes,m}(\lambda_0)$, can be defined from the following equation

$$M(m)V_{mes,m}(\lambda_0) = mV(\lambda_0) + (1-m)V'(\lambda_0), \tag{23}$$

where m is the adaptation coefficient which according to Ref. [13] can be determined from the photopic adaptation luminance and spectral characteristics of the visual adaptation field, $M(m)$ is a normalization function such as the mesopic luminous efficiency $V_{mes,m}(\lambda_0)$ can have a maximum of unity. This mesopic luminous efficiency should be used for the mesopic vision regime where the luminance is approximately between $0.003\,cd/m^2$ and $3\,cd/m^2$. For $m = 1$ the mesopic luminous efficiency becomes the photopic one, $V(\lambda_0)$, while for $m = 0$ it becomes the scotopic one, $V'(\lambda_0)$. The spectral mesopic luminous efficiencies for various values of the adaptation coefficient m are shown in Fig. 15.

The maximum mesopic luminous efficacy $K_{mes,m}$ can be determined from the following equation [13]

$$K_{mes,m} = \frac{683}{V_{mes,m}(\lambda_0 = \lambda_{0,p})}, \qquad \text{lm/W}, \tag{24}$$

where $\lambda_{0,p} = 555\,\text{nm}$, i.e. the peak wavelength of the photopic luminous efficiency. The values of the normalization function $M(m)$ and of the maximum mesopic luminous efficacy $K_{mes,m}$

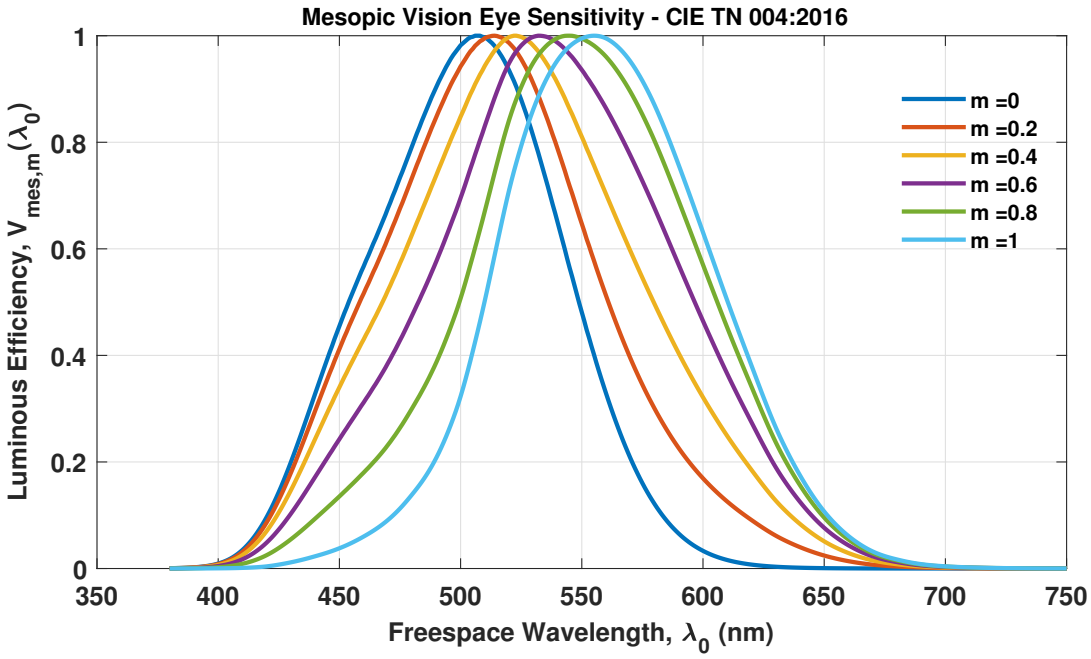

Figure 15: Mesopic luminous efficiency curves for various values of the adaptation coefficient. The $m = 1$ corresponds to photopic luminous efficiency and the $m = 0$ corresponds to the scotopic luminous efficiency.

are shown as functions of the adaptation coefficient m in Figs. 16 and 17, respectively. It can be observed that the maximum mesopic efficacy for $m = 1$ is $683\,lm/W$ and for $m = 0$ is $1700\,lm/W$ respectively, as expected for the photopic and scotopic vision regimes. Finally, the resulting luminous power of a light source in the mesopic regime can be determined by

$$\Phi_v = K_{mes,m}(lm/W)\int_{\lambda_0}\Phi_e(\lambda_0)V_{mes,m}(\lambda_0)d\lambda_0, \qquad \text{Mesopic Vision.} \tag{25}$$

3. Colorimetry Basics

Colorimetry is the field of science and technology that deals with the assessment, quantification, and measurement of color as it is perceived by the human eye. Therefore, in colorimetry, subjective color descriptions are replaced by objective numerical values. The foundations of colorimetry were set in the early nineteenth century with the work of Young, Helmholtz and Maxwell, who recognized the principles of additive and subtractive color mixing, and proposed the trichromatic nature of human color vision. The trichromatic theory is based on the three types of photoreceptors of the human retina and their response to various stimuli. The trichromatic theory is based on the experimental result that almost any color can be

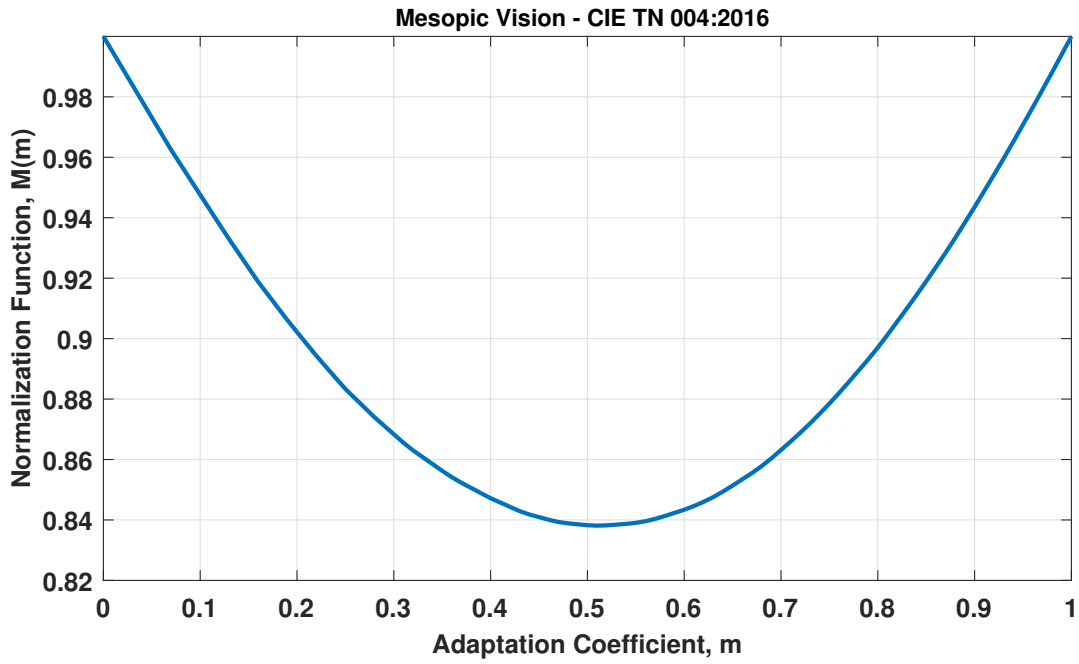

Figure 16: The normalization function $M(m)$ as a function of the adaptation coefficient m.

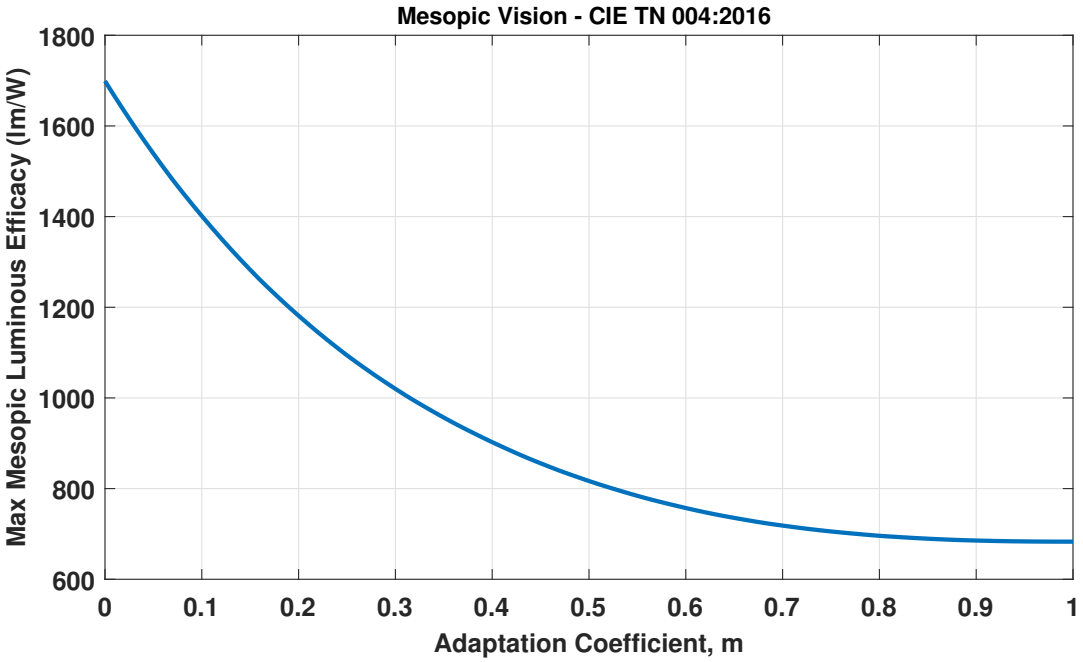

Figure 17: The maximum mesopic efficacy $K_{mes}(m)$ (in lm/W) as a function of the adaptation coefficient m.

reproduced by appropriate mixing of three primary colors (red, green and blue). Most of today's color TV's, computer monitors, color photography, etc. are based on the trichromatic theory [5]. Another competing theory is the opponent-color theory which was proposed by E. Hering in 1878 [5]. This is again based on three types of photoreceptors which respond to red-green, yellow-blue, and white-black opponencies (the previous pairs form the opponent colors) and that any color that is observed by the human eye depends on the response of these opponent-color photoreceptors. In the remainder of this introductory material the trichromatic theory will be followed which is the prevailing one for the time being. The colorimetry as a science has been formalized in 1931 when the International Commission for Illumination (*Commission Internationale de l' Eclairage, CIE*) has standardized the measurement of color by means of color-matching functions and the corresponding chromaticity diagram [15].

3.1. RGB Color Space

In a trichromatic color mixing system color matching functions need to be determined. These are the relative weights of the three primary colors to be used. According to CIE [15, 16] the color matching functions were determined using the following three monochromatic primary colors: $\lambda_R = 700.0\,\text{nm}$ for R (red), $\lambda_G = 546.1\,\text{nm}$ for G (green), and $\lambda_B = 435.8\,\text{nm}$ for B (blue). In addition, as a basic stimulus was considered the white color. The relative amounts of the three primary colors that reproduced the basic white color was 1.0000:4.5907:0.0601 for R, G, and B respectively when photometric units are used. In other words a $1.0000 + 4.5907 + 0.0601 = 5.6508$ lumens of white light can be matched by 1.0000 lumen of R, 4.5907 lumens of G, and 0.0601 lumens of B. In order to establish the color matching functions the measurement system was based on the setup shown in Fig. 18. A test monochromatic light illuminates the test field area. A human observer is able to "make" the two lights appear identical in the comparison field are (color matching) by adjusting the relative intensities of the red (R), green (G), and blue (B) light (the three primaries used). The three color-matching functions are obtained from a series of such matches, in which the human observer sets the intensities of the three primary lights required to match a series of monochromatic lights across the visible spectrum [4]. In case that the monochromatic color can not be matched with the use of the three primaries in the comparison field area, some primary color is added into the test field area by activating some primaries in the test area. This is the case that the relative intensity weighting of the corresponding primary is considered to be negative.

Let $[F]$ the stimulus of a given color [5]. The stimuli of the three primaries are defined as $[R]$, $[G]$, and $[B]$ for red, green, and blue primaries, respectively. Assume the $[F(\lambda_0)]$ is

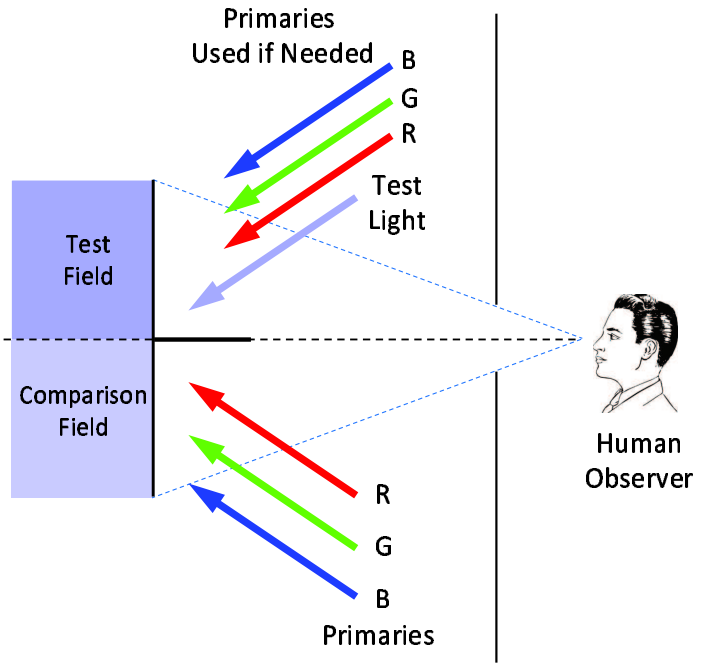

Figure 18: The color matching measurement procedure. A monochromatic test light illuminates the test field. The test light is matched using combination of the three primaries [red (R), green (G), blue (B)] in the comparision field according to the human observer that adjusts the weights of the three primaries. In some cases usage of primaries in the test field is required for matching the test color. This is the case of negative weighting factor of a primary.

the stimulus of the test monochromatic color shown in Fig. 18. Then according to Ref. [5] the following equation can be written

$$[F(\lambda_0)] = \bar{r}(\lambda_0)[R] + \bar{g}(\lambda_0)[G] + \bar{b}(\lambda_0)[B], \tag{26}$$

where $\bar{r}(\lambda_0), \bar{g}(\lambda_0), \bar{b}(\lambda_0)$ are defined as the color matching coefficients at wavelength λ_0. The equality sign of Eq. (26) means that there is a visual match (for the human eye) of the test light (at λ_0) with the linear mixture of the $[R]$, $[G]$, and $[B]$ primaries. In addition, it is assumed that the Grassmann empirical rules of analogy and addition are followed [5]. These are related to the relative intensities of the primaries of Fig. 18. The values of these color matching coefficients are shown in Fig. 19 as functions of the freespace wavelength λ_0 of the test color [15].

Equation (26) can be viewed as a vector equation in three dimensional vector space spanned by $[R]$, $[G]$ and $[B]$ primaries [5]. The three-dimensional space so constructed is used for the geometrical expression of colors and is called a color space. Any color $[F]$ can be located in the color space at the point defined by the matching amounts of $[R]$, $[G]$ and $[B]$, i.e., $[F] = R[R] + G[G] + B[B]$. The R, G, B, matching amounts are defined as the

tristimulus values of stimulus (color) $[F]$. For a light source with power spectrum $P(\lambda_0)$ the R, G, and B tristimulus values can be obtained by the following equations

$$\begin{aligned} R &= k \int_{\lambda_0} \bar{r}(\lambda_0) P(\lambda_0) d\lambda_0, \\ G &= k \int_{\lambda_0} \bar{g}(\lambda_0) P(\lambda_0) d\lambda_0, \\ B &= k \int_{\lambda_0} \bar{b}(\lambda_0) P(\lambda_0) d\lambda_0, \end{aligned} \tag{27}$$

where k is a constant to make R, G, and B dimensionless. The intersection (r, g, b) of the vector $[F]$ and the unit plane $R+G+B=1$ is commonly used to express color $[F]$ according to the following equations

$$\begin{aligned} r &= \frac{R}{R+G+B}, \\ g &= \frac{G}{R+G+B}, \\ b &= \frac{B}{R+G+B}, \end{aligned} \tag{28}$$

where the r, g, b are defined as the rgb chromaticity coordinates. Since $r+g+b=1$ only the two out of the three are necessary to define the color $[F]$ (for example r and g can be used). A diagram showing only the r and g (or any two of the r, g, b) is called chromaticity diagram. Such a diagram for r and g is shown in Fig. 21. The chromaticity coordinates of color $[F]$ correspond to a point inside chromaticity diagram. The chromaticity coordinates for monochromatic light are called spectral chromaticity coordinates and correspond to the contour of the chromaticity diagram of Fig. 21 which also referred as spectrum locus. The straight line connecting the left and right edges of the lobe-shaped curve forms the line of purples. The point $r = g = 1/3 = b$ point is the equal energy white color point. The chromaticity coordinates of any real color are enclosed by the spectrum locus and the line of purples.

3.2. XYZ Color Space

In order to avoid the negative values that the $\bar{r}(\lambda_0)$, $\bar{g}(\lambda_0)$,and $\bar{b}(\lambda_0)$ can attain, CIE published the $\bar{x}(\lambda_0)$, $\bar{y}(\lambda_0)$, $\bar{z}(\lambda_0)$ color matching functions that are greater or equal to zero for any wavelength in the visible spectrum. The three color-matching functions $\bar{x}(\lambda_0)$, $\bar{y}(\lambda_0)$, $\bar{z}(\lambda_0)$ reflect the fact that human color vision possesses trichromacy, that is, the color of any light source can be described by just three variables similarly to the $\bar{r}(\lambda_0)$, $\bar{g}(\lambda_0)$, $\bar{b}(\lambda_0)$ color matching functions. These color matching functions are dimensionless. The $\bar{y}(\lambda_0)$ color matching function was set equal to the photopic luminous efficiency of the human eye, i.e.

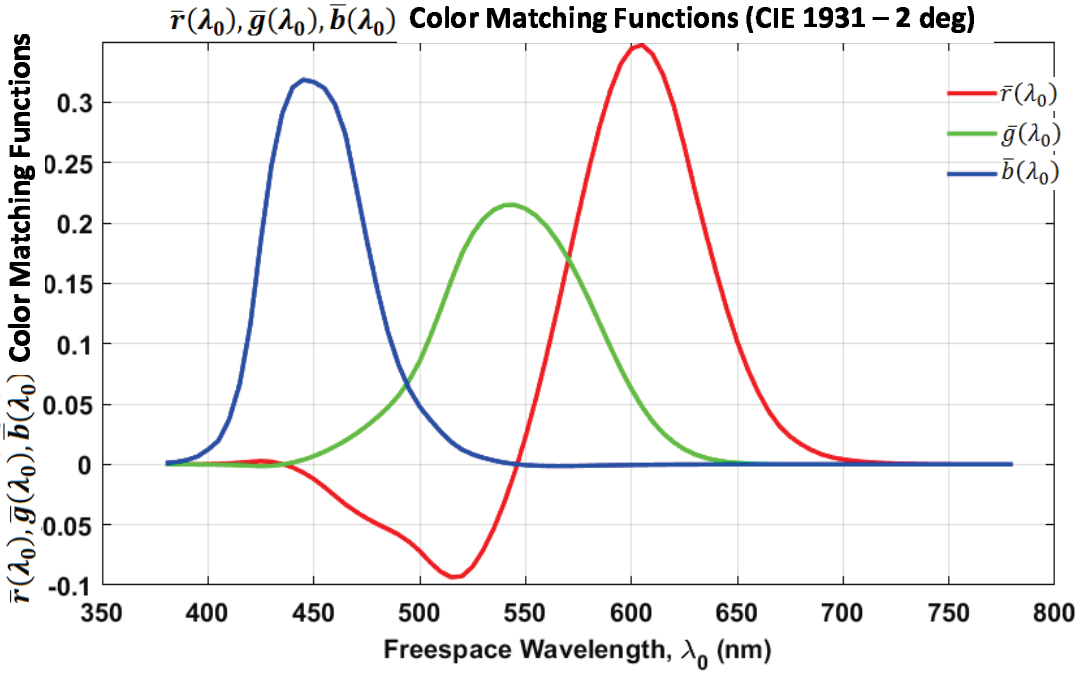

Figure 19: The $\bar{r}(\lambda_0)$, $\bar{g}(\lambda_0)$, $\bar{b}(\lambda_0)$ color matching functions (CIE 1931 - 2 degrees).

$\bar{y}(\lambda_0) = V(\lambda_0)$. The CIE 1931 $\bar{x}(\lambda_0)$, $\bar{y}(\lambda_0)$, $\bar{z}(\lambda_0)$ color matching functions are shown in Fig. 22 [15]. Similarly to Eq. (27) the tristimulus X, Y, Z values for a light source of power spectrum $P(\lambda_0)$ can be defined as

$$\begin{aligned} X &= k \int_{\lambda_0} \bar{x}(\lambda_0) P(\lambda_0) d\lambda_0, \\ Y &= k \int_{\lambda_0} \bar{y}(\lambda_0) P(\lambda_0) d\lambda_0, \\ Z &= k \int_{\lambda_0} \bar{z}(\lambda_0) P(\lambda_0) d\lambda_0, \end{aligned} \tag{29}$$

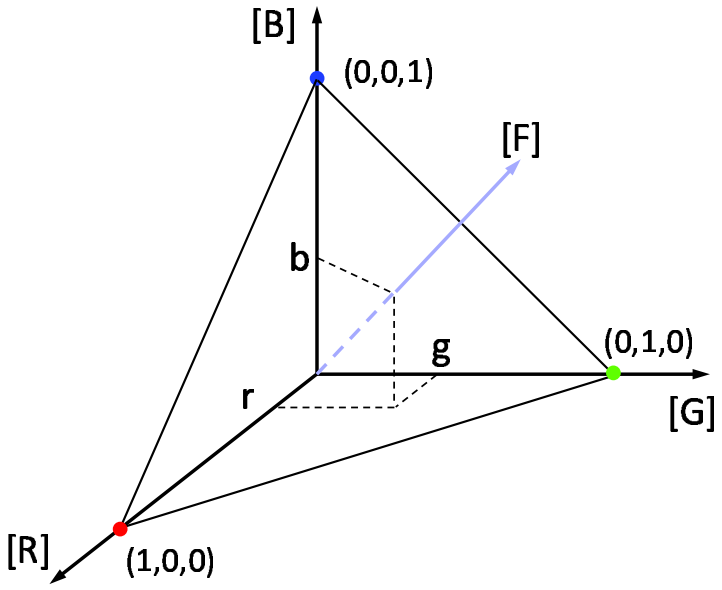

Figure 20: The r, g, b chromaticity coordinates of color stimulus $[F]$.

where k is a constant to make X, Y, and Z dimensionless. Then the corresponding xyz chromaticity coordinates can be defined similarly to rgb by

$$\begin{aligned} x &= \frac{X}{X+Y+Z}, \\ y &= \frac{Y}{X+Y+Z}, \\ z &= \frac{Z}{X+Y+Z}, \end{aligned} \tag{30}$$

Again since $x + y + z = 1$ only two of the chromaticity coordinates (for example x and y) are needed (by convention x and y). It can be shown that for the equal energy white color the tristimulus X, Y, and Z values are related to the tristimulus R, G, and B values by a linear transformation [5, 16]

$$\begin{bmatrix} X \\ Y \\ Z \end{bmatrix} = \begin{bmatrix} 2.768892 & 1.751748 & 1.130160 \\ 1.000000 & 4.590700 & 0.060100 \\ 0 & 0.056508 & 5.594292 \end{bmatrix} \begin{bmatrix} R \\ G \\ B \end{bmatrix}. \tag{31}$$

Because the color matching functions are the tristimulus values of monochromatic light the above transformation holds between $[\bar{x}(\lambda_0), \bar{y}(\lambda_0), \bar{z}(\lambda_0)]$ and $[\bar{r}(\lambda_0), \bar{g}(\lambda_0), \bar{b}(\lambda_0)]$ also.

The CIE chromaticity diagram is shown in Fig. 23. The curved boundary of this shoe-horse-type diagram corresponds to monochromatic colors. The bottom line of the shoe-horse diagram is known as the "line of purples" and there are no real monochromatic color on this

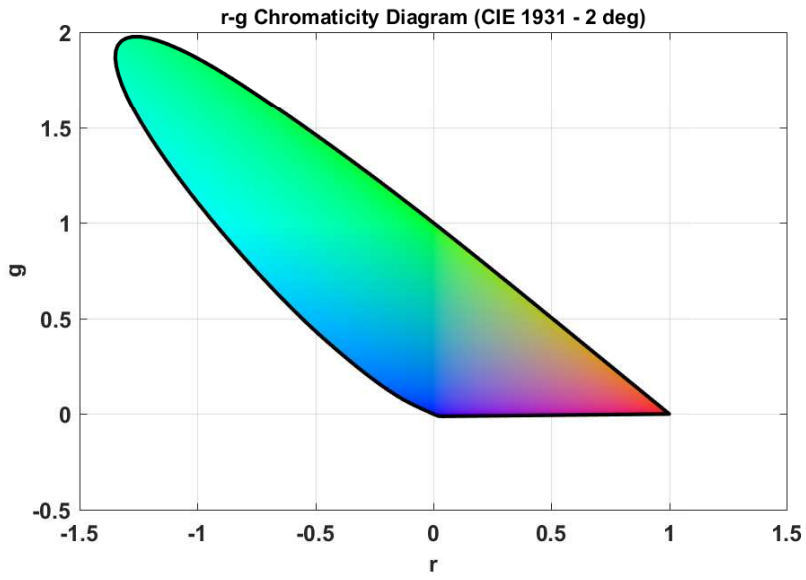

(a)

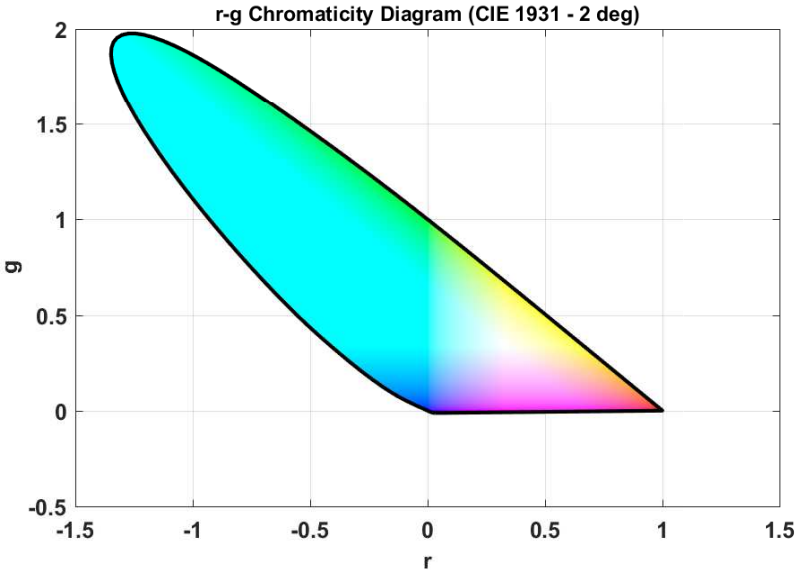

(b)

Figure 21: (a) The CIE r-g chromaticity diagram (from 1931 2-deg data) where the white point has $r = g = b = 1/3$ and its representative color in sRGB standard is determined by $R = G = B = 1/3$. In this case the white point looks grey due to its low illumination and accordingly all other colors in the diagram. (b) Same as (a) but with $R = G = B = 1$ (in sRGB standard) which corresponds to the correctly illuminated white.

line. Any interior point of the diagram specified by the (x, y) chromaticity coordinates represents a color that can be seen by the human eye. White light is found in near the center of the chromaticity diagram. When white light is represented by the $x_w = y_w = z_w =$

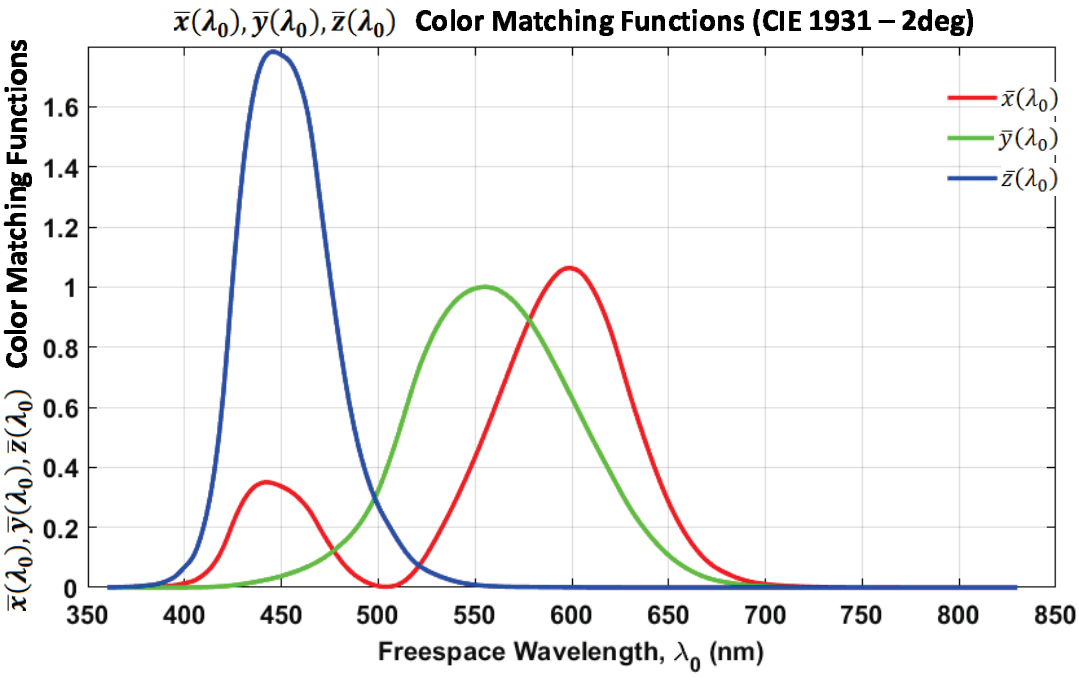

Figure 22: The $\bar{x}(\lambda_0)$, $\bar{y}(\lambda_0)$, $\bar{z}(\lambda_0)$ color matching functions (CIE 1931 - 2 degrees).

1/3 point is called equal-energy-point. However, depending on the white ligth definition other white point locations could be used (assuming the the spectral distribution of the white light source is known). For example for standard RGB color system (sRGB) the D65 illuminant could be used (which assumed blackbody illumination at a temperature of $T = 6504°$ K). In the latter case $x_w = 0.3127$, $y_w = 0.3290$ and $z_w = 0.3583$ correspond to the chromaticity coordinates of the white light. In Fig. 23a the (x, y) chromaticity coordinates were transformed into R, G, B coordinates assuming that $y = Y$ (where Y represents the luminance of the color). In Fig. 23b the luminance was adjusted from the r, g, b values from point to point and looks like a brighter version of Fig. 23a.

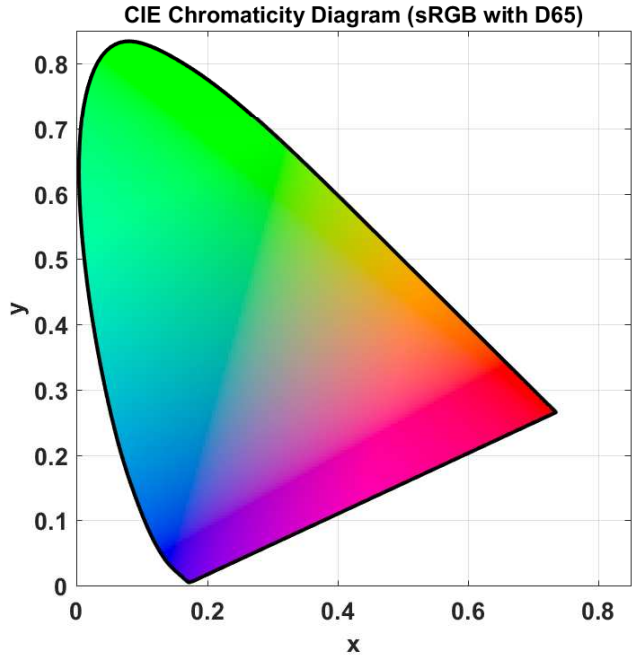

(a)

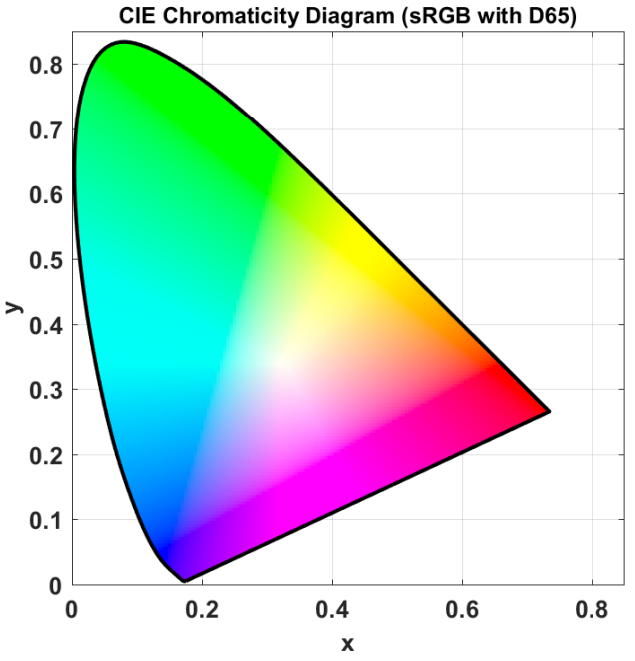

(b)

Figure 23: (a) The CIE chromaticity diagram for $X = x$, $Y = y$, and $Z = z$. (b) The CIE chromaticity diagram for $X = x/w_{max}$, $Y = y/w_{max}$, and $Z = z/w_{max}$ where $w_{max} = \max\{x, y, z\}$.

References

[1] E. T. Zalewski, "Radiometry and photometry," in *Devices, Measurements and Properties* (M. Bass, ed.), Handbook of Optics, , vol. II, ch. 24, New York: McGraw-Hill Inc., 1995.

[2] W. R. McCluney, *Introduction to Radiometry and Photometry*. Boston: Artech House Inc., 1994.

[3] W. L. Wolfe, *Introduction to Radiometry*. Tutorial Texts in Optical Engineering, vol. TT29, Bellingham, WA, USA: SPIE Press, 1998.

[4] E. F. Schubert, *Light Emitting Diodes*. New York: Cambridge University Press, 2nd ed., 2006.

[5] N. Ohta and A. R. Robertson, *Colorimetry: Fundamentals and Applications*. Sussex, UK: J. Wiley & Sons Ltd., 2005.

[6] "Nikon Instruments, Inc., MicroscopyU, the source for microscopy education." https://www.microscopyu.com/tutorials/ccd-signal-to-noise-ratio. Accessed: 2019-03-22.

[7] CIE, *Commission Internationale de l'Eclairage Proceedings (CIE)*. Cambridge, MA: Cambridge University Press, 1926.

[8] K. S. Gibson and E. P. T. Tyndall, "Visibility of radiant energy," *Scientific Papers of the Bureau of Standards*, vol. 19, pp. 131–191, 1923.

[9] CIE *Commission Internationale de l'Eclairage Proceedings (CIE)*, vol. 1, 1951. Sec. 4, vol. 3, p. 37.

[10] Y. LeGrand, *Light, Colour and Vision*. London: Chapman and Hall, 1968.

[11] C. Oleary, *Standards Colorimetry: Definitions, Algorithms and Software*. Sussex, UK: J. Wiley & Sons, Ltd., 2016.

[12] CIE, "Recommended system for mesopic photometry based on visual performance," *Commission Internationale de l'Eclairage Proceedings (CIE)*, 2010. Technical Report 191.

[13] CIE, "The use of terms and units in photometry implementation of the CIE system for mesopic photometry," *Commission Internationale de l'Eclairage Proceedings (CIE)*, 2016. Technical Report 004:2016.

[14] M. Shpak, P. Karha, and E. Ikonen, "Mathematical limitations of the CIE mesopic photometry system," *Lighting Research & Technology*, vol. 49, no. 1, pp. 111–121, 2017.

[15] CIE *Commission Internationale de l'Eclairage Proceedings (CIE)*, 1931.

[16] CIE, "Colorimetry," *Commission Internationale de l'Eclairage Proceedings (CIE)*, 2004. Technical Report CIE:15:2004.